

# Peptide-Based Probes with Artificial Anion Binding Motif for Direct Fluorescence ‘Switch-On’ Detection of Nucleic Acid in Cells

Debabrata Maity,<sup>[a]</sup> Marija Matković,<sup>[b]</sup> Shang Li,<sup>[c]</sup> Martin Ehlers,<sup>[a]</sup> Junchen Wu,<sup>[c]</sup> Ivo Piantanida,<sup>[b]\*</sup> and Carsten Schmuck<sup>[a]\*</sup>

**Abstract:** We report two new peptide based fluorescence probes **1** and **2** for the detection of ds-DNA at physiological pH. **1** and **2** contain amino-naphthalimide and diethyl-aminocoumarin fluorophores, respectively, with two identical peptide arms each equipped with a guanidiniocarbonylpyrrole (GCP) artificial anion-binding motif. **1** and **2** show ‘switch-on’ fluorescence response upon binding to ds-DNA, whereby they can differentiate between various types of polynucleotides. For instance they exhibit more pronounced fluorescence response for AT-rich polynucleotides than GC-rich polynucleotides, and both give only negligible response to ds-RNA. The fluorimetric response of **1** is proportional to the AT-basepair content in DNA, while the fluorescence of **2** is sensitive to secondary structure of polynucleotide. Fluorescence experiments, thermal melting experiments and circular dichroism studies reveal that **1** interacts with ds-DNA in a combined intercalation and minor groove binding, while **2** interacts mainly with the outer surface of DNA/RNA. As **1** and **2** have a very low cytotoxicity, **1** can be applied for the imaging of nuclear DNA in cells.

## Introduction

The development of highly sensitive and selective probes to detect double-stranded DNA (ds-DNA) is very crucial for biological studies, clinical diagnostics, gene therapy and biodefense applications.<sup>1</sup> Fluorescence as a highly sensitive, relatively rapid and easy to operate approach has attracted significant interest in nucleic acid detection. These qualities open up opportunities for researchers to design promising reagents for the diagnosis of genetic diseases and the monitoring of biological processes in cells.<sup>2</sup> There are some

classic fluorescent DNA dyes (e.g., ethidium bromide,<sup>3</sup> TOTO,<sup>4</sup> Sybr Green,<sup>5</sup> [Ru(phen)<sub>2</sub>dppz]<sup>2+</sup>,<sup>6</sup> DAPI and Hoechst dyes<sup>7</sup>) which mainly bind to DNA by intercalation or groove binding. Often Molecular beacons (MBs), synthetic oligonucleotides end-labelled with two fluorophores, are used to recognize their complementary DNA strand. In recent times, some other approaches were reported in this area like pyrene-functionalized oligonucleotides and locked nucleic acid,<sup>8</sup> quencher-free MBs,<sup>9</sup> wavelength-shifting MBs,<sup>10</sup> and MBs based on excimer fluorescence colour readout,<sup>11</sup> based on peptide nucleic acids.<sup>12</sup> However, cell permeability of these imaging agents is very poor and often they fail to enter cells directly. Additional artificial transfection vectors are then required for imaging of nucleic acids in cells. We recently developed a lysine containing peptide beacon with two pyrenes as chromophores for ratiometric detection of nuclear DNA by fluorescence microscopy.<sup>13a</sup> Upon binding to nucleic acids, this peptide beacon underwent conformational changes within the minor groove resulting in significant changes of the fluorescence properties. However, pyrene as chromophore does have some disadvantages. As part of a larger program in our laboratory aimed at developing receptors and probes for anionic biomolecules such as amino acid,<sup>14</sup> peptides and proteins,<sup>15</sup> nucleotides and nucleic acids,<sup>13b,16</sup> glycosaminoglycans,<sup>17</sup> lipopolysaccharide<sup>18</sup> etc. using ion pair interactions, we sought to devise novel methods for monitoring nucleic acid in biological fluids. In this paper, we report two new peptide based nucleic acid probes **1** and **2**, containing aminonaphthalimide and diethylaminocoumarin fluorophores respectively for fluorescence ‘switch-on’ detection of nucleic acids at physiological pH (Figure 1). Those probes contain two identical peptidic arms which are equipped with a lysine and an additional artificial anion-binding moiety, a guanidiniocarbonyl pyrrole cation (GCP). The increase in emission intensity ( $I/I_0$ ) upon interaction with nucleic acids varies for different types of polynucleotides. Maximum fluorescence intensity is observed when they bind to AT-rich DNA. It seems that **1** interacts with ds-DNA in a combined intercalation and minor groove binding mode, while **2** interacts only with the outer surface of DNA/RNA. **1** and **2** are found to be non-toxic. Furthermore, **1** can be applied for imaging of nuclear DNA in cells, using fluorescence microscopy, without the need of any additional transfection vectors to facilitate cell uptake.

[a] Dr. D. Maity, Dr. M. Ehlers, Prof. Dr. C. Schmuck  
Institute of Organic Chemistry  
University of Duisburg-Essen  
45117 Essen, Germany  
E-mail: Carsten.schmuck@uni-due.de

[b] S. Li, Prof. Dr. J. Wu  
Key Lab for Advanced Materials and Institute of Fine Chemicals  
East China University of Science and Technology  
200237 Shanghai, China

[b] M. Matković, Dr. I. Piantanida  
Ruđer Bošković Institute  
HR-10000 Zagreb, Croatia

## Results and Discussion

**Design and Synthesis.** The structure of peptidic probes **1** and **2** is very flexible hopefully enabling them to bind to DNA (Figure 1). They consist of two identical peptidic arms, each attached via the C-terminus to a central highly flexible spacer. Each arm includes as head group, a guanidinocarbonylpyrrole (GCP) moiety, an anion-binding site developed by our working group.<sup>19</sup> It is very effective in binding oxoanions by means of a salt bridge strengthened by multiple hydrogen bonds even under physiological conditions. The central spacer is tagged with a fluorophore as reporter unit which should exhibit significant changes in fluorescence properties upon DNA binding. Specifically, **1** and **2** contain 4-morpholine-1,8-naphthalimide and 7-(diethylamino)coumarin as fluorophores, respectively. The emission property of these fluorophores is highly sensitive to their immediate environment. Normally they exhibit very weak fluorescence in polar and protic environments but show strong and blue-shifted emission in hydrophobic surroundings.<sup>20</sup> Additionally, each side chain consists of one lysine for additional charge-charge interactions with the phosphate backbone of DNA. Free cationic probes **1** and **2** are expected to be weakly fluorescent but fluorescence should be turned-on when they bind to ds-DNA. As depicted in Scheme 1, the syntheses of **1** and **2** were carried out by means of microwave-assisted solid-phase peptide synthesis on Fmoc-Rink-Amide resin. For the synthesis of **1**, rink amide 4-methylbenzhydrylamine (MBHA) resin (0.8 mmol/g) was swelled in DCM and Fmoc-Lys(Alloc)-OH was attached as a spacer to the solid support under argon atmosphere with PyBOP as coupling reagent in 5% DIPEA/DMF using three equivalents of each reactant. With the help of a single-mode microwave, the reaction mixture was irradiated for 20 min at 20 W and allowed to reach a maximum temperature of 60 °C. The coupling step was repeated to assure complete conversion of all accessible amino groups on the resin. After the removal of the Alloc protecting group using Pd(PPh<sub>3</sub>)<sub>4</sub> (0.1 eq) and PhSiH<sub>3</sub> (24 eq) in DCM (room temperature, 20 min), the N- $\alpha$ -Fmoc-(4-morpholine-1,8-naphthalimido)-lysine<sup>18</sup> was coupled. After deprotection of the Fmoc group with 20% piperidine/DMF (1+5 min, 20 W, max. 60 °C), lysine and the tert-butoxycarbonyl (Boc)-protected guanidinocarbonylpyrrole (GCP) were coupled similarly using six equivalents of each reactant. For the synthesis of **2**, rink amide MBHA resin (0.8 mmol/g) was swelled in DCM, Fmoc-Lys(Alloc)-OH was attached as a spacer to the solid support. After the removal of the Alloc protecting group, again Fmoc-Lys(Alloc)-OH was coupled. After the removal of the Alloc protecting group, the 7-(diethylamino)coumarin-3-carboxylic acid was coupled. After deprotection of the Fmoc group, lysine and the Boc-protected GCP motif were coupled similarly using six equivalents of each reactant. Finally, resins were thoroughly washed and dried and the probe was cleaved from the solid support; the Boc-protected side chains were deprotected at the same time without microwave irradiation by utilizing a cleavage mixture composed of trifluoroacetic acid (TFA) / water / triisopropylsilane (TIS) (95:2.5:2.5). After purification probe **1** and **2** were obtained as hydrochloride salt.

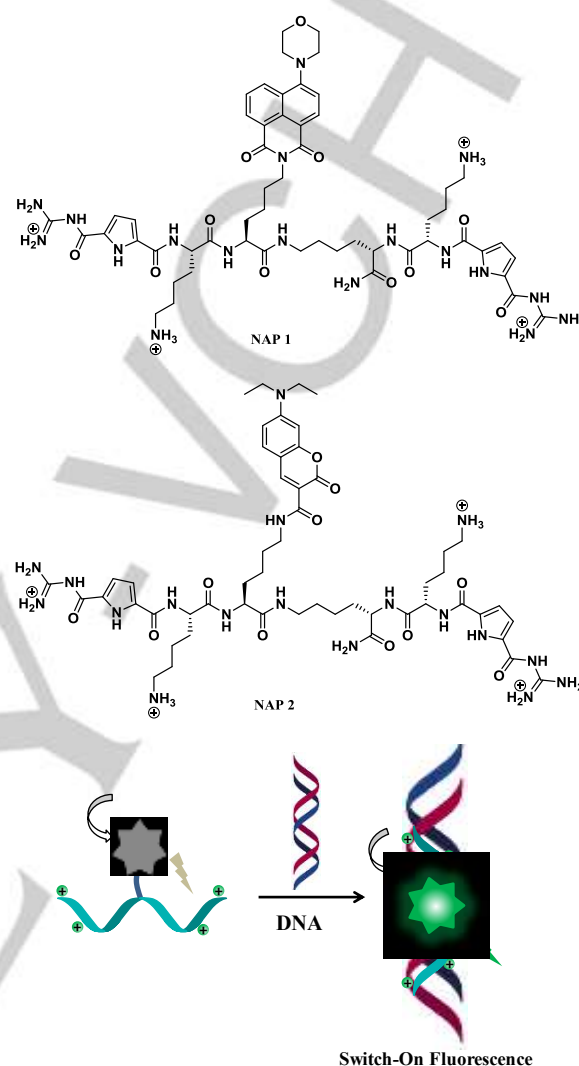
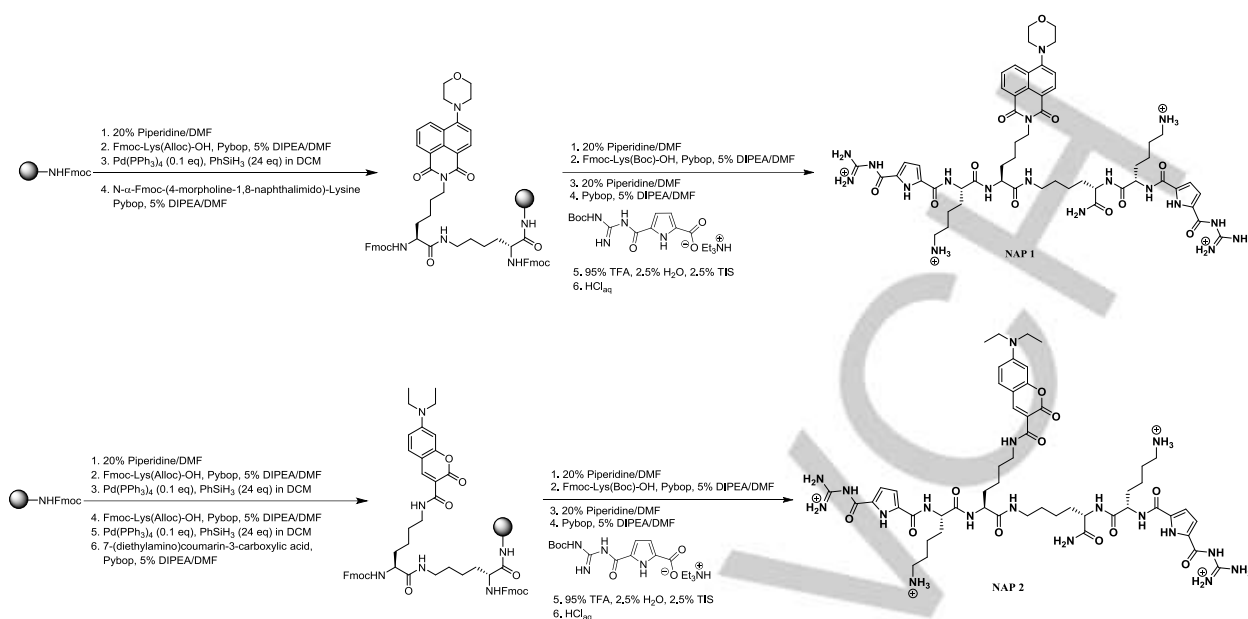


**Figure 1.** Molecular structure of **1** and **2** and cartoon representation their interaction with nucleic acid.

**Binding Studies.** Firstly, we performed calibration and checked stability of both peptides. The absorbance of aqueous solutions of both peptide **1** and **2** are proportional to their concentrations (Figure S1 and S3 in the SI). Hence, no significant intermolecular aggregation of the compounds occurred in the concentration range studied. Aqueous solutions of both peptides were stable, not showing any signs of decomposition upon standing for several days at room temperature or upon heating to 95 °C for at least 1 hour (Figure S2 and S4 in the SI). Therefore, we have carried out nucleic acid binding studies with both peptides. According to the previously published  $pK_a$  value of our GCP group (ca. 6-7) the protonation state of **1** and **2** at neutral conditions is +2 due to the protonated lysine, while at pH 5 both compounds have 4 positive charges due to additional



**Scheme 1.** Microwave assisted SPPS of the probes **1** and **2**.

protonation of the GCP moiety.<sup>21</sup> **1** showed a very weak fluorescence emission at 550 nm upon 410 nm excitation in neutral aqueous conditions (sodium cacodylate buffer,  $I = 0.05$  M, pH 7.2). **2** also showed a weak fluorescence emission at 476 nm upon 430 nm excitation in neutral aqueous conditions (sodium cacodylate buffer,  $I = 0.05$  M, pH 7.2).

A remarkable fluorescence enhancement was observed as shown in Figure 2, when p(dA·dT)<sub>2</sub> was added to the solution of **1**. Upon sequential addition of p(dA·dT)<sub>2</sub>, the fluorescence intensity is increased by more than 10-fold, and the emission spectrum is blue-shifted to 530 nm. These fluorescence enhancements vary with the different type of polynucleotides used for titration (Figure 3). Maximum fluorescence was observed for p(dA·dT)<sub>2</sub> and significantly lower fluorescence was observed for p(dG·dC)<sub>2</sub> and pApU even at higher dye concentration (Figure S5 in the SI). Calf-thymus DNA (ctDNA) having ca. 52% AT and 48% GC showed a moderate response (6-fold). Results show a direct correlation between the fluorescence emission increase and AT-basepair content. Therefore, the relative emission intensity ( $I/I_0$ ) at 550 nm can be used for 'switch-on' detection of p(dA·dT)<sub>2</sub> or even estimation of the AT-basepairs in mixed DNA sequences (ct-DNA) since the difference in response is proportional to the AT-basepair content in ct-DNA (Figure 3).

Addition of p(dA·dT)<sub>2</sub> also increases fluorescence of **2** much stronger than GC-DNA or AU-RNA (Figure 4). However, for ct-DNA the emission increase is stronger than expected based on the AT-basepair content. Since AT-DNA and ct-DNA are both typical B-DNA helices, GC-DNA is characterized by severely restricted minor groove (due to protruding amino groups), and AU-RNA is A-helix<sup>26</sup>, it seems that the fluorescence increase of **2** can be attributed to sensing of the secondary structure of double helix<sup>26</sup> and not to the AT-basepair content.

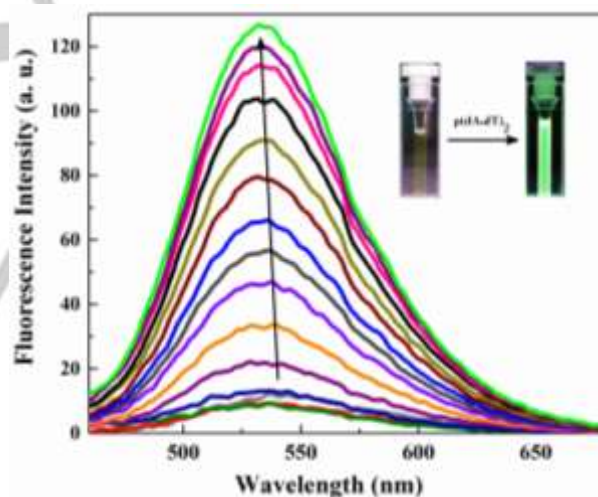


**Figure 2.** Fluorescence emission spectra for the titration of a 0.5  $\mu$  M solution of **1** with increasing concentration of p(dA·dT)<sub>2</sub> in sodium cacodylate buffer ( $I = 0.05$  M, pH 7.2). ( $\lambda_{ex} = 410$  nm). Inset: Fluorescence switched-on after addition of ds-DNA inside cuvette.

Comparative fluorimetric experiments (Figures 3 and 5) were performed at the same experimental conditions to express in the best way the selectivity of fluorimetric response. However, such conditions did not allow the accurate titrations for low-responsive polynucleotides (GC-DNA, AU-RNA), therefore to determine the binding constants we have repeated all fluorimetric titrations of nucleic acids with **1** and **2** under optimal experimental conditions for non-linear fitting procedures to Scatchard equation<sup>22</sup> (Figure S7-S14 in the SI). Processing of fluorimetric data yielded values

of ratio  $n_{[\text{bound dye}]/[\text{polynucleotide}]}$  vary  $\pm 0.1$ , corresponding values of binding constant  $K$  varying up to 30%. Comparison of obtained data revealed moderate affinity of **1** or **2** to the studied DNA/RNA, whereby the affinity of **1** is somewhat higher for  $p(\text{dA}\cdot\text{dT})_2$  ( $\log K = 4.6$ ) than for  $p(\text{dG}\cdot\text{dC})_2$  ( $\log K = 3.8$ ). At variance to **1**, **2** shows similar binding affinity towards all studied DNAs ( $\log K = 4.7$  and  $\log K = 4.8$  respectively for  $p(\text{dA}\cdot\text{dT})_2$  and  $p(\text{dG}\cdot\text{dC})_2$ ). However for both probes, slightly weaker binding was observed with ds-RNA (polyA–polyU) ( $\log K = 3.8$  and  $\log K = 4.4$  respectively for **1** and **2**). Thus, although the affinity of **1**, **2** is only marginally selective toward AT-DNA in respect to GC-DNA and AU-RNA, fluorimetric selectivity is much more pronounced, pointing out to the importance of fluorophore positioning within the polynucleotide binding site.

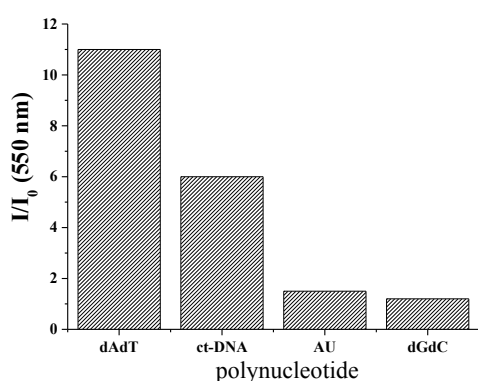


**Figure 3.** Fluorimetric response of **1** ( $0.5 \mu\text{M}$ ) upon binding to  $p(\text{dA}\cdot\text{dT})_2$ , ctDNA, pApU and  $p(\text{dG}\cdot\text{dC})_2$  in sodium cacodylate buffer ( $I = 0.05 \text{ M}$ ,  $\text{pH } 7.2$ ). ( $\lambda_{\text{ex}} = 410 \text{ nm}$ ). All titrations were done under the same instrument setup. Relative emission intensity  $I/I_0$  ( $I_0$  = fluorescence intensity of solution containing free compound at 550 nm,  $I$  = fluorescence intensity of solution with compound-polynucleotide complex at 550 nm).

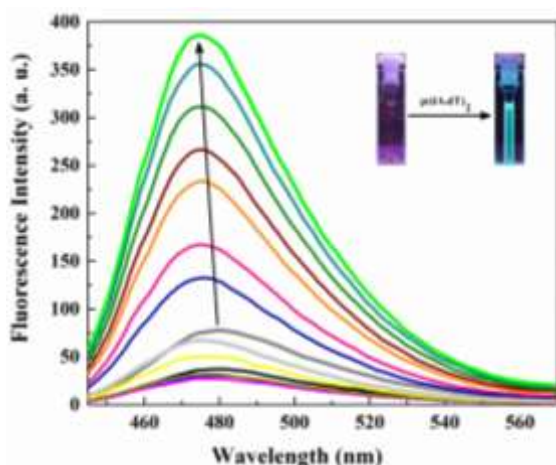


**Figure 4.** Fluorescence emission spectra for the titration of a  $0.5 \mu\text{M}$  solution of **2** with increasing concentration of  $p(\text{dA}\cdot\text{dT})_2$  in sodium cacodylate buffer ( $I = 0.05 \text{ M}$ ,  $\text{pH } 7.2$ ). ( $\lambda_{\text{ex}} = 430 \text{ nm}$ ). Inset: Fluorescence switched-on after addition of ds-DNA inside cuvette.

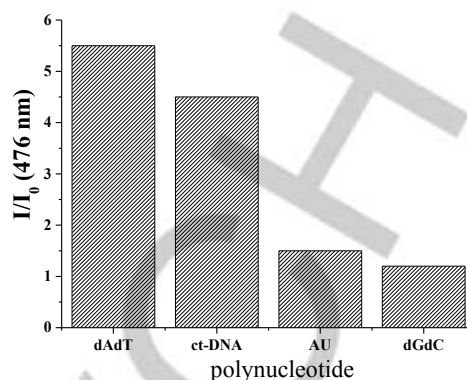


**Figure 5.** Fluorimetric response of **2** ( $0.5 \mu\text{M}$ ) upon binding to  $p(\text{dA}\cdot\text{dT})_2$ , ctDNA, pApU and  $p(\text{dG}\cdot\text{dC})_2$  in sodium cacodylate buffer ( $I = 0.05 \text{ M}$ ,  $\text{pH } 7.2$ ). ( $\lambda_{\text{ex}} = 430 \text{ nm}$ ). All titrations were done under the same instrument setup. Relative emission intensity  $I/I_0$  ( $I_0$  = fluorescence intensity of solution containing free compound at 476 nm,  $I$  = fluorescence intensity of solution with compound-polynucleotide complex at 476 nm).

Then, we checked thermal stabilisation of dsDNA-**1** and dsDNA-**2** complexes by temperature-dependent UV-vis absorption studies (Figure S15-S19, Table S5 in the SI). Probe **1** bound to  $p(\text{dA}\cdot\text{dT})_2$  and ctDNA yielded increase in DNA melting temperatures ( $T_m$ ) with  $\Delta T_m = 7.4$  and  $2.0$  at ratio  $r_{[\text{compound}]/[\text{polynucleotide}]} = 0.3$ , respectively. A significant increase in  $T_m$  of **1**/  $p(\text{dA}\cdot\text{dT})_2$  complex in respect to mixed sequence 1/ ct-DNA complex provided additional evidence for selective response of **1** to AT-base rich regions of DNA, which agreed well with aforementioned fluorimetric selectivity.

Addition of **2** to  $p(\text{dA}\cdot\text{dT})_2$  increased the melting temperatures ( $T_m$ ) only by  $\Delta T_m = 1$  and did not show any influence on the  $T_m$  value of ct-DNA at  $r = 0.3$ . The effects of **1** and **2** on ds-RNA (polyA–polyU) were negligible.

Such pronounced differences in emission selectivity, as well as thermal denaturation impact toward various DNA and RNA required more detailed structural analysis of fluorophore/polynucleotide binding mode. For that purpose we applied CD spectropolarimetry (Figure S20-24 in the SI), as a highly sensitive method for conformational changes in the secondary structure of polynucleotides.<sup>23</sup> Moreover, small achiral chromophores which bind to DNA / RNA a way uniformly oriented in respect to polynucleotide chiral axis, will acquire an induced CD spectrum  $> 300 \text{ nm}$  (where DNA/RNA does not have CD spectrum), whereby ICD band sign and intensity are directly correlated to chromophore binding mode. For instance, intercalation usually yields weak negative ICD band, groove binding gives strong positive ICD band, while agglomeration along DNA/RNA results in bisignate ICD bands.<sup>24b</sup> Studied compounds **1**, **2** are chiral and thus have intrinsic CD spectra in UV range  $< 220 \text{ nm}$ ; however chromophores in UV/vis range  $> 300 \text{ nm}$  are not directly attached to the chirality centre and thus do not show any CD band. Therefore, the intrinsic CD spectra of the compounds do not interfere with the region used to study interactions with DNA and RNA ( $230 - 500 \text{ nm}$ ).

Taking into account the binding constants determined from fluorimetric titrations ( $\log K = 3.8-4.8$ ), in CD experiments ( $20 \mu\text{M}$  DNA/RNA, ratio  $r_{[\text{dye}]/[\text{polynucleotide}]} = 0.1-0.9$ ) the percentage of dye/polynucleotide complex formed is 35-90%, which should be sufficient for monitoring the structural changes in CD spectra of DNA/RNA. Moreover, molar extinction coefficients of **1**, **2** (Figures S1, S2) are high enough to provide eventual induced (I)CD bands  $> 300 \text{ nm}$  as a result of DNA/RNA binding.

In general, successive additions (ratio  $r_{[\text{dye}]/[\text{polynucleotide}]} = 0.1-0.9$ ) of **1** to any DNA or RNA resulted in pronounced changes of CD spectra of polynucleotides, causing even sign inversion of DNA/RNA positive bands (about 260-280 nm) into strongly negative ones. Such effects support efficient complex formation with strong effect on DNA/RNA secondary structure. However, since both, polynucleotide and **1** absorb light in 240-300 nm range, and taking into account that intensity and sign of **1** ICD band is not possible to predict, observed effects cannot be accurately deconvoluted in contributions of DNA/RNA structure change and eventual ICD band of **1**. Fortunately, positive induced CD band at 300-330 nm (Figure 6), could be attributed solely to GCP unit positioning within the DNA minor groove.<sup>21,24b</sup> Such positive ICD band  $> 300 \text{ nm}$  was not observed for **1**/RNA complex (Figure S23 in the SI), which is in accordance with our previous results that neither of RNA grooves is an appropriate binding site for the GCP unit.<sup>21,26</sup> Intriguingly no ICD band was observed within the wavelength range of amino-naphthalimide chromophore of **1**, suggesting either non-uniform positioning of that moiety in respect to polynucleotide chiral axis or partial intercalation between base pairs at an angle that additionally decreases commonly weak negative band of intercalators.<sup>24b</sup>

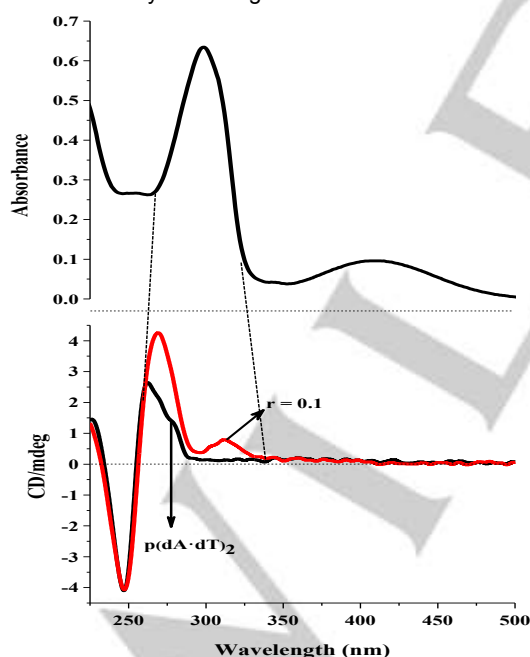


**Figure 6.** Top: UV/Vis spectrum of **1**. Down: CD spectrum of free  $p(\text{dA}\cdot\text{dT})_2$  ( $30 \mu\text{M}$ ) and complexed with **1** at molar ratio  $r_{[\text{1}]/[\text{polynucleotide}]} = 0.1$  in sodium cacodylate buffer ( $I = 0.05 \text{ M}$ ,  $\text{pH } 7.2$ ).

At variance to naphthalimide **1**, diethyl-aminocoumarin analogue **2** did not cause any change in CD spectrum of any studied DNA/RNA (Figure S24 in the SI), and didn't yield any significant ICD band. That could be correlated to much weaker thermal stabilization effects of **2** to ds-DNA, thus suggesting that binding of **2** does not influence the secondary structure of polynucleotide significantly, whereby chromophores (GCP, diethyl-aminocoumarin) are not uniformly oriented along polynucleotide chiral axis. Thus, main interaction of **2** with DNA/RNA could be based on non-specific electrostatic interactions of positively charged lysines and GCP unit with polynucleotide backbone, combined with hydrophobic interactions of diethyl-aminocoumarin within grooves.

All results suggest that the difference between **1** and **2** is based on chromophore positioning in the DNA or RNA complex, whereby naphthalimide due to the larger aromatic surface seems to at least partially intercalate between basepairs, at variance to smaller and more sterically hindered diethyl-aminocoumarin, which is located by hydrophobic interactions non-specifically and poorly oriented within DNA or RNA grooves. Molecular modelling calculations (Schrödinger version 9.8, OPLS forcefield, water solvation model) (Figure 7) also supported for **1** that naphthalimide can intercalate into the base pairs of  $p(\text{dA}\cdot\text{dT})_2$ , while GCP can additionally interact by H-bonding and electrostatic interactions (as noted by ICD band, Figure 6). In addition, AT-DNA has a well-defined, properly spaced, and easily accessible minor groove,<sup>26</sup> which can accommodate hydrophobic fluorophores,<sup>25</sup> such as GCP unit.<sup>21</sup> In contrast, GC-rich DNA has a minor groove sterically more crowded due to the protruding amino groups of the guanine base.<sup>26</sup> Finally, RNA has very shallow and broad minor groove, while its major groove is much deeper than DNA, neither of these supporting efficient binding of molecules which fit into DNA minor groove.<sup>26</sup>

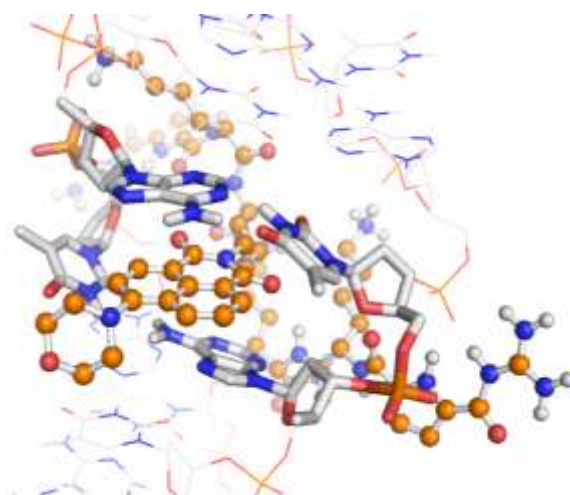


**Figure 7.** A possible binding mode of **1** to  $p(\text{dA}\cdot\text{dT})_2$  according to molecular modelling calculations.

**Cell imaging of nuclear DNA.** Such fluorimetric selectivity and in particular strong enhancement of fluorescence upon DNA binding prompted us to study fluorescence imaging properties of **1** and A549 cells using confocal laser scanning microscopy (CLSM) (Figure 8). The cells were treated with **1**. Fluorescent images of individual fixed cells clearly showed strong green fluorescence signal coming from the nucleus. There was no fluorescence observed from the cytoplasm. So, **1** is capable of entering the cell, reaching the nucleus, and binding to the nucleic acids, which gives rise to a strong green fluorescence. An extraordinarily high signal-to-background ratio between the nucleus (>1000) and the cytoplasm was quantified from luminescence intensity plot, indicating exclusive staining of the cell nucleus (spot 2). Colocalization studies with DAPI, a well-established dye for DNA staining in the nucleus, further confirmed that **1** was found only in the nucleus of the cell. Hence, **1** is capable of entering the cells and stains the nuclear DNA. As often cytotoxicity is a major problem with DNA binding probes, cell toxicity of **1** and **2** toward the A549 cell line was measured using a standard MTT assay (Figure S25 in the SI). At **1** and **2** concentrations of 0.5–8.0  $\mu\text{M}$ , cell viabilities were found to be greater than 90% after incubation for 24 h suggesting very low toxicity of both the probes.

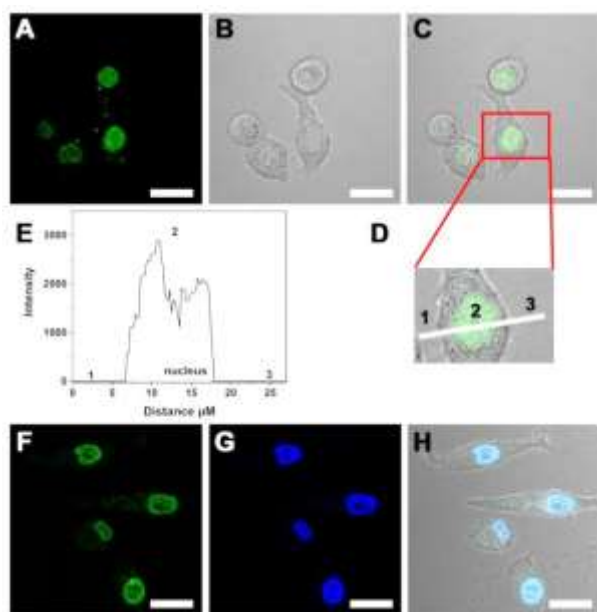


**Figure 8.** (A–C) CLSM images of A549 cells incubated with **1** in RPMI 1640 medium (6.0  $\mu\text{M}$ ) for 30 min at 37 °C. (B) and (C) are bright-field and overlay images of (A), respectively. (D) Amplified imaging of one cell [red square in (C)]. (E) Cross-sectional analysis (along the white line in image D) indicated that the luminescence stems exclusively from the nucleus (spot 2) and not from the cytoplasm (spot 3). (F–H) CLSM images of (F) A549 cells incubated for 30 min at 37 °C with **1** in RPMI 1640 medium (6  $\mu\text{M}$ ) and (G) A549 cells fixed by MeOH and then stained with DAPI (1  $\mu\text{g/mL}$ ) in RPMI 1640 medium for 6 h at 37 °C with 5%  $\text{CO}_2$ ; (H) is the overlay image of (F), (G), and the corresponding bright-field image (Channel 1 for DAPI: excitation: 405 nm, emission collected: 424–454 nm; Channel 2 for **1**: excitation: 405 nm, emission collected: 534–594 nm; Scale bar is 20  $\mu\text{m}$ ).

## Conclusions

In conclusion, we have successfully designed and prepared two oligopeptides **1** and **2**, which can be used as fluorescence “switch-on” probes for ds-DNA. The key feature of these probes is to use environment-sensitive fluorophores, coupled with a artificial strong anion binding site, the guanidincarbonylpyrrole (GCP) moiety. Fluorescence experiments, thermal melting experiments and circular dichroism studies reveal that **1** interacts with ds-DNA in a combined intercalation and minor groove binding mode, while **2** interacts only with the outer surface of DNA/RNA. The remarkable ‘switch-on’ fluorescence signal of **1** and to some extent **2** also can be used to differentiate different types of polynucleotides, as they exhibited significantly more pronounced fluorescence response for AT-rich polynucleotides than GC-rich polynucleotides, while simultaneously being almost non-responsive to ds-RNA. In that respect, **1** showed also fluorimetric response proportional to AT-basepair content in DNA, while for its close analogue **2** fluorescence was sensitive to the secondary structure of polynucleotide. The utility of **1** as a bioanalytical molecular tool has also been demonstrated by fluorescence imaging upon binding to nuclear DNA, whereby both, **1** and **2** showed very low cytotoxicity.

## Experimental Section

For experimental Details see Supporting Information.

## Acknowledgements

IP and MM thank the Croatian Science Foundation project 1477, FP7-REGPOT-2012-2013-1, Grant Agreement Number 316289 – InnoMol for financial support.

**Keywords:** molecular recognition • fluorescent probe • DNA detection • cell imaging • anion receptors

- [1] [a] Hurley, L. H. *Nat. Rev. Cancer*. **2002**, *2*, 188–200. [b] Balasubramanian, S. L.; Hurley, H.; Neidle, S. *Nat. Rev. Drug Discov.* **2011**, *10*, 261. [c] Wilson, W. D.; Tanious, F. A.; Mathis, A.; Tevis, D.; Hall J. E.; Boykin, D. W. *Biochimie*, **2008**, *90*, 999.
- [2] [a] Armitage, B. A. *Top. Curr. Chem.* **2005**, *253*, 55–76. [b] Ranasinghe, R. T.; Brown, T. *Chem. Commun.* **2005**, 5487–5502. [c] Waring, M. J. *Annu. Rev. Biochem.* **1981**, *50*, 159–192.
- [3] [a] LePecq, J. B.; Paoletti, C. A. *J. Mol. Biol.* **1967**, *27*, 87–106. [b] Dragan, A. I.; Bishop, E. S.; Strouse, R. J.; Casas-Finet, J. R.; Schenerman, M. A.; Geddes, C. D. *Chem. Phys. Lett.* **2009**, *480*, 296–299. [c] Wei, B.; Li, H.; Dong, S. *Chem. Commun.* **2007**, 73–75.
- [4] Chiang, C. K.; Huang, C. C.; Liu, C. W.; Chang, H. T. *Anal. Chem.* **2008**, *80*, 3716–3721.
- [5] Wang, J.; Liu, B. *Chem. Commun.* **2008**, 4759–4761.
- [6] [a] Friedman, A. E.; Chambron, J. C.; Sauvage, J. P.; Turro, N. J.; Barton, J. K. *J. Am. Chem. Soc.* **1990**, *112*, 4960–4962. [b] Jenkins, Y.; Barton, J. K. *J. Am. Chem. Soc.* **1992**, *114*, 8736–8738. [c] Jiang, Y.; Fang, X.; Bai, C. *Anal. Chem.* **2004**, *76*, 5230–5235. [d] Wang, J.; Jiang, Y.; Zhou, C.; Fang, X. *Anal. Chem.* **2005**, *77*, 3542–3546.

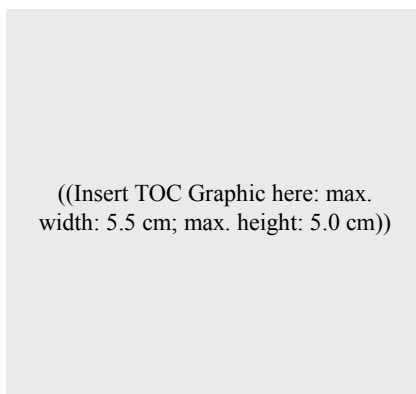
- [7] [a] Zhu, Z.; Yang, C.; Zhou, X.; Qin, J. *Chem. Commun.* **2011**, 47, 3192–3194. [b] Zhu, Z.; Xu, L.; Zhou, X.; Qin, J. Yang, C. *Chem. Commun.* **2011**, 47, 8010–8012.
- [8] Østergaard, M. E.; Hrdlicka, P. J. *Chem. Soc. Rev.* **2011**, 40, 5771–5788.
- [9] [a] Hwang, G. T.; Seo, Y. J.; Kim, H. B. *J. Am. Chem. Soc.* **2004**, 126, 6528–6529. [b] Venkatesan, N.; Seo, Y. J.; Kim, H. B. *Chem. Soc. Rev.* **2008**, 37, 648–663.
- [10] [a] Socher, E.; Jarikote, D. V.; Knoll, A.; Röglin, L.; Burmeister, J.; Seitz, O. *Anal. Biochem.* **2008**, 375, 318–330. [b] Socher, E.; Berthge, L.; Knoll, A.; Jungnick, N.; Herrmann, A.; Seitz, O. *Angew. Chem. Int. Ed.* **2008**, 47, 9555–9559.
- [11] [a] Berndt, S.; Wagenknecht, H.-A. *Angew. Chem. Int. Ed.* **2009**, 48, 2418–2421. [b] Häner, R.; Biner, S. M.; Langenegger, S. M.; Meng, T.; Malinovskii, V. L. *Angew. Chem. Int. Ed.* **2010**, 49, 1227–1230. [c] Hara, Y.; Fujii, T.; Kashida, H.; Sekiguchi, K.; Liang, X.; Niwa, K.; Takase, T.; Yoshida, Y.; Asanuma, H. *Angew. Chem. Int. Ed.* **2010**, 49, 5502–5506. [d] Kashida, H.; Takatsu, T.; Fujii, T.; Sekiguchi, K.; Liang, X.; Niwa, K.; Takase, T.; Yoshida, Y.; Asanuma, H. *Angew. Chem. Int. Ed.* **2009**, 48, 7044–7047. [e] Holzhauser, C.; Wagenknecht, H. A. *Angew. Chem. Int. Ed.* **2011**, 50, 7268–7272.
- [12] [a] Kummer, S.; Knoll, A.; Socher, E.; Bethge, L.; Herrmann, A.; Seitz, O. *Angew. Chem. Int. Ed.* **2011**, 50, 1931–1934. [b] Vasilyeva, E.; Lam, B.; Fang, Z.; Minden, M. D.; Sargent, E. H.; Kelley, S. O. *Angew. Chem. Int. Ed.* **2011**, 50, 4137–4141.
- [13] [a] Wu, J.; Zou, Y.; Li, C.; Sicking, W.; Piantanida, I.; Yi, T.; Schmuck, C. *J. Am. Chem. Soc.* **2012**, 134, 1958–1961. [b] Maity, D.; Jiang, J.; Ehlers, M.; Wu, J.; Schmuck, C.; *Chem. Commun.* **2016**, 52, 6134–6137.
- [14] [a] Schmuck, C. *Chem. Commun.* **1999**, 843–844. [b] Schmuck, C.; Geiger, L. *J. Am. Chem. Soc.* **2005**, 127, 10486–10487. [c] Maity, D.; Schmuck, C. *Synthetic Receptors for Amino Acids and Peptides*, *Royal Society of Chemistry*, **2015**, 8, 326–368.
- [15] [a] Schmuck, C.; Geiger, L. *J. Am. Chem. Soc.* **2004**, 126, 8898–8899. [b] Wich, P. R.; Schmuck, C. *Angew. Chem. Int. Ed.* **2010**, 49, 4113–4116.
- [16] [a] Kuchelmeister, H. Y.; Schmuck, C. *Chem.—Eur. J.* **2011**, 17, 5311–5318. [b] Maity, D.; Li, M.; Ehlers, M.; Schmuck, C. *Chem. Commun.*, **2017**, 53, 208–211.
- [17] Maity, D.; Schmuck, C. *Chem.—Eur. J.* **2016**, 22, 13156–13161.
- [18] Wu, J.; Zawistowski, A.; Ehrmann, M.; Yi, T.; Schmuck, C. *J. Am. Chem. Soc.* **2011**, 133, 9720–9723.
- [19] [a] Schmuck, C. *Chem. Eur. J.* **2000**, 6, 709–718. [b] Schmuck, C.; Heil, M.; Baumann, K.; Scheiber, J. *Angew. Chem. Int. Ed.* **2005**, 44, 7208–7212.
- [20] [a] Lakowicz, J. R. *Principles of Fluorescence Spectroscopy*, 3<sup>rd</sup> ed., *Springer*, New York, **2006**. [b] Loving, G. S.; Sainlos, M.; Imperiali, B. *Trends Biotechnol.* **2010**, 28, 73–83.
- [21] Hernandez-Folgado, L.; Baretic, D.; Piantanida, I.; Marjanovic, M.; Kralj, M.; Rehm, T.; Schmuck, C. *Chem. Eur. J.* **2010**, 16, 3036–3056.
- [22] Liu, Y.; Kumar, A.; Depauw, S.; Nhili, R.; Cordonnier, M. H. D.; Lee, M. P.; Ismail, M. A.; Farahat, A. A.; Say, M.; Catoen, S. C.; Parra, A. B.; Neidle, S.; Boykin D. W.; Wilson, W. D. *J. Am. Chem. Soc.* **2011**, 133, 10171–10183.
- [23] Rodger, A.; Norden, B. *Circular Dichroism and Linear Dichroism*, Oxford University Press: New York, Chap. 2, **1997**.
- [24] [a] Berova, N.; Nakanishi, K.; Woody, R. W. *Circular Dichroism Principles and Applications*, 2nd ed., New York Wiley-VCH, **2000**. [b] Eriksson, M.; Nordén, B. *Methods Enzymol.* **2001**, 340, 68–98.
- [25] [a] Neidle, S. *Nat. Prod. Rep.* **2001**, 18, 291–309. [b] Dervan, P.B. *Bioorg. Med. Chem.* **2001**, 9, 2215–2235. [c] Narayanaswamy, N.; Das, S.; Samanta, P. K.; Banu, K.; Sharma, G. P.; Mondal, N.; Dhar, S. K.; Pati, S. K.; Govindaraju, T. *Nucl. Acids Res.* **2015**, 43, 8651–8663.
- [26] Cantor, C. R.; Schimmel, P. R., *Biophysical Chemistry*. WH Freeman and Co., San Francisco: 1980; Vol. 3.

**Entry for the Table of Contents** (Please choose one layout)

Layout 1:

**FULL PAPER**

Text for Table of Contents

*Author(s), Corresponding Author(s)\****Page No. – Page No.****Title**

Layout 2:

**FULL PAPER**

((Insert TOC Graphic here; max. width: 11.5 cm; max. height: 2.5 cm))

*Author(s), Corresponding Author(s)\****Page No. – Page No.****Title**

Text for Table of Contents